Molecular Imaging Mass Spectrometry

KUI – 9/2009
Received December 8, 2008
Accepted April 3, 2009

Dj. Josić[a,c] *and S. Kovač*[a,b]

[a] Sveučilište J. J. Strossmayera u Osijeku, Odjel za kemiju, Kuhačeva 20, 31000 Osijek, Hrvatska

[b] Prehrambeno-tehnološki fakultet Osijek, Kuhačeva 18, 31000 Osijek, Hrvatska

[c] Proteomics Core, Center for Cancer Research Development, Rhode Island Hospital and Brown University, Providence, Rhode Island, USA

Molecular imaging mass spectrometry (IMS) is a recently developed method for direct determination of spatial distribution of biopolymers, preferably proteins on cell surface and tissues. Imaging mass spectrometry data are mainly based on Matrix-Assisted Laser Desorption/Ionization – Time of Flight (MALDI TOF). The MALDI TOF based imaging mass spectrometry was applied for determination of changes in kidney tissue of sensitive mice after poisoning with aristolochic acid I. The second application presented here were changes in the gastric tissue in mice after infection with *Helicobacter pylori*, as a model of gastric cancer in humans caused by this pathogen microorganism. Molecular imaging mass spectrometry can be applied in medicine, mostly for identification of candidate biomarkers for malignant and non-malignant diseases. Furthermore, imaging MS has almost unlimited capacity in agriculture, food technology and biotechnology, e. g. for monitoring, process development and quality control of manufactured tissue of animal, plant and microbial origin.

Key words: *Imaging mass spectrometry, aristolochic acid, nephropathy, gastric cancer, biomarkers*

Introduction

Developments in mass spectrometry in the last twenty years allow analysis of solid state materials and numerous applications have emerged in diverse fields such as biotechnology, medicine, microelectronics, material science, geochemistry and surface analysis (Reviewed in Reference 1). The increasing interest in imaging mass spectrometry is due to its ability for parallel detection of multiple analytes, gathering of exact molecular masses at the same time to record spatial distributions of a wide range of small molecules, but also large biopolymers such as proteins and polysaccharides, and to perform the analyses on native samples without labelling. Structural data can also be obtained by performing MS/MS.[2] Additionally, continuing improvements in all these aspects, in software and hardware of the instrument are the reason for increasing interest in this method.

Molecular Imaging Mass Spectrometry

The possibility of direct determination of the spatial distribution of chemical components in cells and tissues makes imaging mass spectrometry extremely interesting for applications in biology, biotechnology and medicine. With an appropriate sample preparation, images of distributions of small molecules, drugs and other organic compounds, but also images of macromolecular components and structures such as proteins, carbohydrates and lipids can be obtained.[1–3] Most imaging mass spectrometry data are based either on Matrix-Assisted Laser Desorption/Ionization (MALDI) or Secondary Ion Mass Spectrometry (SIMS).[2,4] These two techniques offer different capabilities. MALDI can record the spatial distribution of high mass molecules, e. g. proteins using the specific molecular ions. Typical spatial resolution is about 25 μm, but recently 10 μm sources are available. SIMS is able to provide high spatial resolution images in the sub-micron range.[2,5] There are some impressive applications of SIMS for the imaging of small molecules[1,5,6] but the molecular ion mass range of this technique is much lower than that of MALDI, and most imaging experiments use ions of $m/z < 500$.[2] The m/z range for MALDI is one to two orders of magnitude higher, and that is why it is the method of choice for recording intact polypeptide and protein distributions. By use of this method, proteins can be analyzed directly from tissue sections, and their distribution can be determined.[3,7,8] The overview of the imaging mass spectrometry experiment is shown in Fig. 1.

Molecular imaging spectrometry can be applied for pathological studies and for biomarker analysis.[3,7–10] It has been applied to investigate proteome changes in different tumors such as glioblastoma,[3] colon tumors,[11] liver metastasis,[12] in Alzheimer disease,[10] in nefrotoxicity induced by antibiotics,[13] during mouse prostate development,[9] nervous tissue[14] etc. There are two approaches for direct tissue mass spectral analysis: "profiling" or "imaging". Molecular imaging MS is the acquisition of complete mass spectra from each spot on the surface of the analyte (e. g. tissue section, plant leaf, other organic or inorganic materials) without knowing about the structure of the molecules desorbed and ionised. Molecular profiling MS is the acquisition of a part or a small m/z region of a mass spectrum from each spot on

[*] Presented in part at the XII. Ružička Days, Vukovar, Croatia, September 18–19, 2008.

the surface of the analyte knowing the structure of the molecules desorbed and ionised, i. e. searching for the ion with a particular *m/z* value across the surface. Molecular imaging and profiling is nowadays mostly done with cluster ions as a primary beam because these beams generate sufficient secondary molecular ions.[1–3]

For imaging mass spectrometry, sample preparation is a key step in the analytical procedure.[3,14,15] Any molecular degradation, or other reaction, e. g. protein–protein interaction and/or aggregation that occurs in the time between sample collection and analysis can influence the results. Samples can be prepared using several protocols such as direct analysis of frozen sections,[3,16] isolation of individual cells by laser-capture microdissection or contact blotting of a tissue on a membrane target.[17] The most used method is the application of the tissue section onto a gold coated or stainless steel target plate, coating with a matrix solution, drying and introduction into the MALDI mass spectrometer.[2,3,18] Corresponding software for the instrument control and evaluation is commercially available. Molecular images are created from a raster over the surface of the sample with consecutive laser spots. The image resolution depends on the number of spots. The molecular mass range is between 500 and 80000. However, the upper limit for lower abundant proteins is about 30000 D (for method description cf. References 2, 3 and 18). There are new instruments being developed to improve spatial resolution, molecular sensitivity and speed of the analysis. The high-resolution images on the order of 10 μm[18,19] and down to 4 μm[20] are reported, but these instruments are still in the early stage of development.[18]

A direct comparison between the protein and peptide distribution and cellular morphology determined by histology is an important step on the path to the discovery of cell specific biomarkers.[21] The compatibility of several well-established tissue staining protocols with the MALDI MS analyses has already been demonstrated.[21]

Application

Kidneys from aristolochic acid treated mice

Aristolochic acid (AA) present in *Aristolochia* plants are toxins responsible for Chinese Herbs Nephropathy (CHN). This type of rapidly progressive interstitial renal fibrosis reported in a group of Belgian women after the introduction of medicaments based on Chinese herbs.[22] The disease is characterized by early, severe anemia and mild tubular proteinuria, and renal interstitial fibrosis. Urothelial malignancy

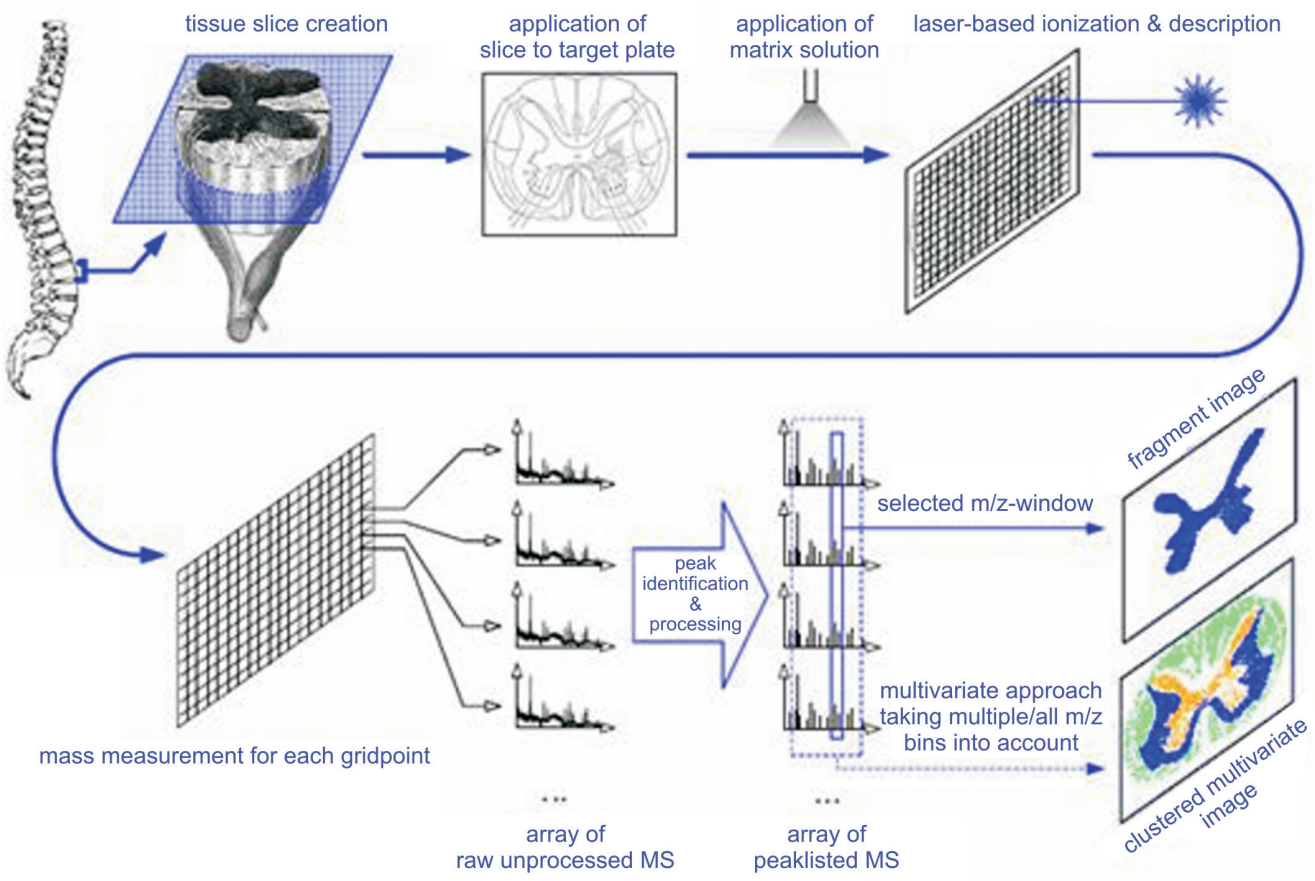

F i g. 1 – *Overview of the imaging mass spectrometry experiment using MALDI TOF MS (Taken from:* Van de Plas *et al. (2007) Pacific Symp. on Biocomputing 12:458-469.)*

S l i k a 1 – *Prikaz eksperimenta "imaging mass spectrometry" uz uporabu MALDI TOF MS (Preuzeto iz: Van de Plas et al. (2007) Pacific Symp. on Biocomputing 12:458-469.)*

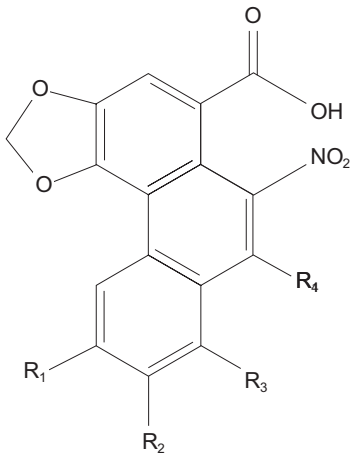

F i g. 2 – *Aristolochic acid (AA)*
AA I: $R_1 = R_2 = R_4 = H$, $R_3 = OCH_3$
AA II: $R_1 = R_2 = R_3 = R_4 = H$

S l i k a 2 – *Aristolohijska kiselina (AA)*
AA I: $R_1 = R_2 = R_4 = H$, $R_3 = OCH_3$
AA II: $R_1 = R_2 = R_3 = R_4 = H$

of the upper urinary tract develops subsequently in almost half of the patients. Exposure to AA was confirmed by the detection of AA-DNA adducts in the kidney tissue samples

from CHN patients.[23] Recently, *Grollman* et al.[24] presented strong indications, that dietary poisoning by AA is also responsible for Endemic (Balkan) nephropathy (EN) and associated urothelial cancer. This renal disease affects the rural population of Southeastern Europe, in Bosnia and Herzegovina, Bulgaria, Croatia, Serbia and Romania.[25] The main features of human CHN, renal intestinal fibrosis and urothelial malignancy have also been reproduced in rats.[26] *Sato* and coworkers[27] reported that mice belonging to the sensitive C3H/He strain, when treated with AA rapidly developed nephropathy. AA is a mixture of structurally related nitrophenanthrene carboxylic acids, containing two major components – aristolochic acid I (AA I) and aristolochic acid II (AA II) (see Ref. 28 and Fig. 2). Investigation using purified AA I and AA II revealed that AA I induced strong nephrotoxicity in mice, and that AA II resulted in mild nephrotoxicity. The other investigated components, AA IVa and aristolactam proved as nontoxic.[27]

Gastric carcinogenesis induced by *H. pylori*

Prior infection with *H. pylori* is the most important risk factor for the development of gastric cancer. Dr. Steven Moss from the Department of Gastroenterology, Rhode Island Hospital, Providence, RI, USA developed p27-deficient mouse model, sensitive to *H. pylori* infection. The p27 protein is a cell cycle regulator and it has been postulated as a link between chronic *H. pylori* infection and gastric cancer.[29] The development of this mouse model of *H. pylori* induced gastric cancer provides an important step forward in dissecting pathogenesis of gastric cancer. The pattern of protein changes in gastric epithelial cells of p27-deficient mice was followed by molecular imaging mass spectrometry.

Experimental

Animal model

Mouse model, introduced by *Sato* at al.[27] was used to compare the effects of two forms of AA: AA I and AA II. The animals were treated with AA (1.8 mg kg^{-1} day^{-1}, i. p.) for 11 days and sacrificed. The histochemistry was performed by Dr. Paul McMillan (CORE Laboratory, Rhode Island Hospital, Providence, RI).

P27-deficient mice were bred, housed and infected with *H. pylori* as previously described[29], and sacrificed after 15 weeks, the time point that corresponds to the start of mild chronic gastritis. Uninfected control p27-deficient mice were euthanized at the same time point as control. At necropsy the stomach was removed and split longitudinally into 3 equal portions for (1) formalin fixation and embedding in paraffin for routine histology (Hematoxylin and Eosin staining), (2) quantitative assessment of *H. pylori* burden, and (3) frozen sectioning for molecular imaging mass spectrometry.*

Sample preparation and molecular imaging mass spectrometry

Sample preparation and histochemistry were performed by Dr. Paul McMillan (CORE Laboratory, Rhode Island Hospital, Providence, RI). Mouse kidneys were harvested and immediately frozen in liquid nitrogen. Tissue sectioning of the frozen sample was carried out using a cryostat. Tissue sections ranging from 5 μm to 15 μm were mounted onto the surface of an electrically conductive ITO glass slide (Bruker Corp. Billerica, MA, USA) and allowed to adhere to the surface simply by surface tension. Tissue sections were rinsed to remove salts by a $t = 30$ s immersion in $\varphi = 70$ % ethanol followed by $\varphi = 96$ % ethanol rinse for $t = 30$ s. The organic matrix sinapinic acid (Sigma Aldrich, St. Louis, MO, USA) which is required for the ionization of molecular signals was applied to the tissue surface automatically with the ImagePrep (Bruker Corp.). The matrix mass concentration of $\gamma = 10$ mg mL^{-1} was dissolved in $\varphi = 60$ % acetonitrile containing $\varphi = 0.2$ % trifluoroacetic acid (Sigma Aldrich). The ImagePrep consumed approximately 2.5 mL of the matrix, which completely covered the glass slide containing multiple tissue sections. During this critical event of matrix deposition, molecules within the tissue are extracted and incor- porated into the matrix layer. Liquid droplets generated with the ImagePrep are on average $\overline{d} = 25$ μm in diameter, which therefore limits the experimental imaging resolution to this droplet size when considering de-localization of molecules within liquid droplet.

The mass analysis was performed with the Ultaflex III™ MALDI TOF MS instrument (Bruker Corp.) configured with the smartbeam™ laser having a beam focus set at 30 μm. The mass range was scanned in linear mode from 600 Da to 30 kDa at a repetition rate of 200 Hz. For all tissue sections, data was collected at a pixel resolution between 75–100 μm.

* The experiments were performed in Dr. Steven Moss' Laboratory (Rhode Island Hospital).

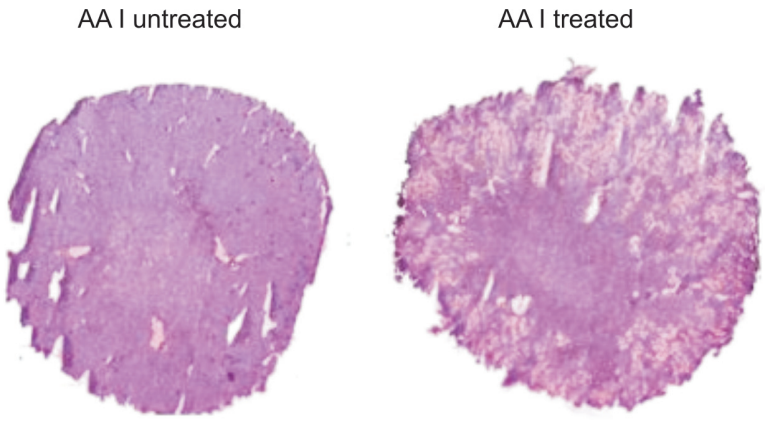

F i g. 3 – *Histological image of mouse kidney after removal of MALDI-matrix, Hematoxylin and Eosin staining, original magnification 10×. Left – control, right – AA I treated.*

S l i k a 3 – *Histološka slika mišjega bubrega nakon uklanjanja MALDI-matriksa, bojeno hematoksilinom i eozinom, uvećanje 10×. Lijevo – kontrola, desno – tretiran s AA I.*

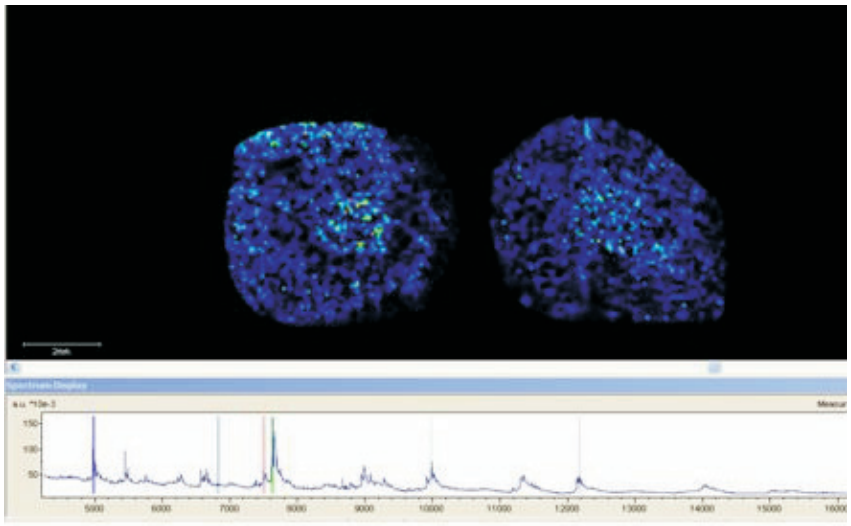

F i g. 4 – *Molecular mass spectrometric imaging of mouse kidney. Left – control, right – AA I treated. Upper part – distribution of the ion with a* m/z *value of* m/z *= 7,791 (corresponding to the molecular ion of a large peptide/small protein). Lower part – Full positive ion MALDI mass spectrum*

S l i k a 4 – *Molekulski maseno-spektrometrijski prikaz mišjega bubrega. Lijevo – kontrola, desno tretiran s AA I. Gornji dio – raspodjela iona s m/z = 7.791 (odgovara molekulskom ionu velikoga peptida ili niskomolekulskog proteina). Donji dio – Kompletan MALDI maseni spektar.*

Results

Mouse kidneys treated with AA

Already after the second day of the treatment, kidneys of AA I sensitive mice show change in histological pattern (see Fig. 3). Molecular image of same tissue is shown in Fig. 4. After application of appropriate matrix and laser-based ionization, molecules are flying towards detector. The time-of-flight of the molecules depends on their mass of fragment and charge (*m/z* value, see lower part of Fig. 3). After scanning of the complete surface of the specimen and analysis by corresponding software, a molecular image for a defined m/z value can be constructed (for the *m/z* = 7,791, see upper part of Fig. 4). Distribution of peaks with three different *m/z* values (1,495; 3,751 and 4,979 respectively) is given in Fig. 5. As shown in the two last figures (Figs. 4 and 5), distribution of these molecules is different in kidneys of AA I treated and AA I untreated mice.

Mouse gastric mucosa after infection with H. pylori

Fig. 6 shows digital images of gastric mucosa of control and *H. pylori* infected mice. MALDI molecular imaging of same specimens shows significant changes in distribution of two proteins with *m/z* values of 9,962 and 14,047 (Fig. 7). As shown in the upper part of Fig. 7, the protein with the *m/z* value of 9,962 is almost completely absent in the mucosa of infected mice. It can be anticipated that studies with this cutting-edge, new technology will help dissect the cellular pathways altered during human gastric carcinogenesis caused by this pathogenic bacteria and define novel biomarkers of risk and prognosis in gastric cancer.

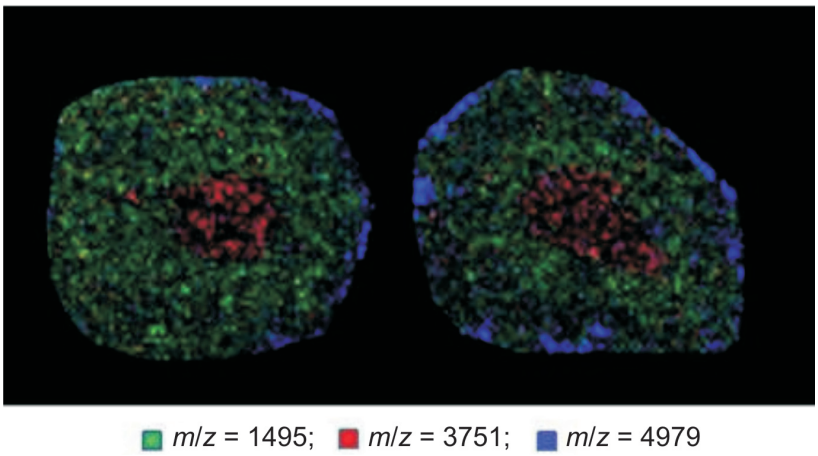

F i g. 5 – *Molecular mass spectrometric image of mouse kidney. Spatial distribution of ions with the following m/z values: 1,495, 3,751 and 4,979 (corresponding presumably to molecular ions of peptides or small proteins). Left – control, right – AA I treated. Upper part – distribution of peaks with different* m/z *values.*

S l i k a 5 – *Molekulski maseno-spektrometrijski prikaz mišjega bubrega. Prostorna raspodjela iona s m/z veličinama: 1.495, 3.751 i 4.979 (za molekulske iona peptida ili niskomolekulskih proteina). Lijevo – kontrola, desno tretiran s AA I. Gornji dio – raspodjela pikova s različitim vrijednostima m/z.*

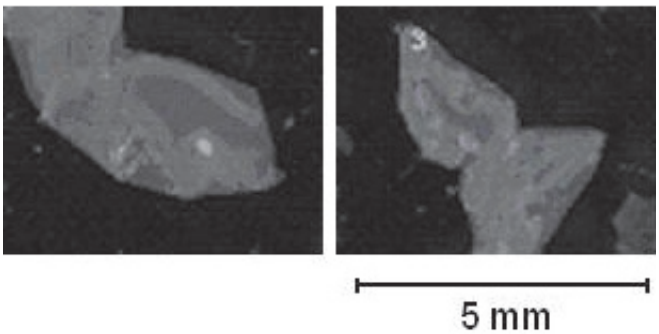

F i g. 6 – *Digital images of mouse gastric mucosa. Left – control, right – 15 weeks after* H. pylori *infection*

S l i k a 6 – *Digitalni prikaz mukoze želuca u miša. Lijevo – kontrola, desno – 15 tjedana nakon infekcije s H. pylori.*

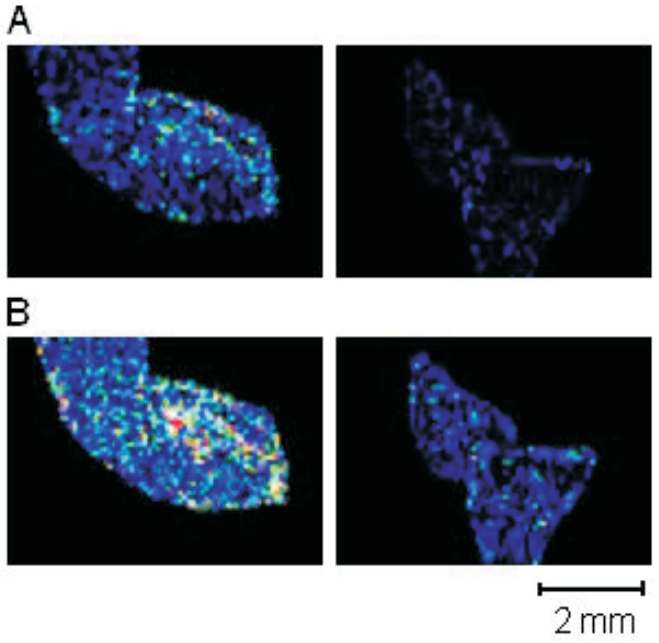

F i g. 7 – *Molecular mass spectrometric image of mouse gastric mucosa. Spatial distribution of ions with the following m/z values: 9,962 (upper part) and 14,047 (lower part, both corresponding presumably to molecular ions of proteins). Left – control, right – 15 weeks after H. pylori infection.*

S l i k a 7 – *Molekulski maseno-spektrometrijski prikaz mukoze želuca u miša. Prostorna raspodjela iona s iznosima m/z: 9.962 (gornji dio) i 14.047 (donji dio, u oba slučaja za molekulske ione proteina). Lijevo – kontrola, desno 15 tjedana nakon infekcije s H. pylori.*

Conclusions

– Molecular imaging is an emerging technique between histopathology and mass spectrometry.

– This technique is now applied in medicine, mostly for identification of candidate biomarkers for several malignant and non-malignant diseases.

– Furthermore, this technique has also almost unlimited capacity for application and biomaterial characterization in food technology and biotechnology, mostly for process development and quality control of manufactured tissue of animal and plant origin.

References:
Literatura:

1. *M. L. Pocholski, N. Winograd,* Chem. Rev. **99** (1999) 2977.
2. *L. A. McDonell, R. M. A. Heeren,* Mass Spectrom. Rev. **26** (2007) 606.
3. *M. Stoeckli, P. Chaurand, D. E. Hallahan, R. M. Caprioli,* Nature Medicine **7** (2001) 493.
4. *P. J. Todd, R. T. Short, C. C. Grimm, W. M. Holland, S. P. Markey*, Anal. Chem. **64** (1992) 1871.
5. *A. M. Kleinfeld, J. P. Kampf, C. Lechene,* J. Am. Soc. Mass Spectrom. **15** (2004) 1572.
6. *S. G. Ostrowski, C. T. Van Bell, N. Winograd, A. G. Ewing,* Science **305** (2004) 71.
7. *R. L. Caldwell, R. M. Caprioli*, Mol. Cell Proteomics **4** (2005) 394.
8. *P. Chaurand, S. Fouchécourt, B. B DaGue, B. J. Xu, M. L Reyzer, M.-C. Orgebin-Crist, R. M. Caprioli*, Proteomics **3** (2003) 2221.
9. *P. Chaurand, M. A. Rahman, P. Hunt, J. A. Mobley, G. Gu, J. C. Latham, R. M. Caprioli, S. Kasper*, Mol. Cell Proteomics **7** (2008) 411.
10. *T. C. Rohner, D. Staab, M. Stoeckli,* Mech. Ageing Dev. **126** (2005) 177.
11. *P. Chaurand, B. B. DaGue, R. Scott Pearsall, D. W. Threadgill, R. M. Caprioli,* Proteomics **1** (2001) 1320.
12. *S. Shimma, M. Setou*, J. Mass Spectrom. Soc. Jpn **55** (2007) 145.
13. *H. Meistermann, J. L. Norris, H. R. Aerni, D. S. Cornett, A. Friedlein, A. R. Erskine, A. Augustin, M. C. De Vera Mudry, S. Ruepp, L. Suter, H. Langen, R. M. Caprioli, A. Ducret,* Mol. Cell Proteomics **5** (2006) 1876.
14. *E. B. Monroe, J. C. Jurchen, B. A. Koszczuk, J. L. Losh, S. S. Rubakhin, J. V. Sweedler*, Anal. Chem.**78** (2006) 6826.
15. *Y. Sugiura, S. Shimma, M. Setou,* J. Mass Spectrom. Soc Jpn **54** (2006) 45.
16. *L. L. Moroz, R. Gillette, J. V. Sweedler*, J. Exp. Biol. **202** (1999) 333.
17. *P. Chaurand, M. Stoeckli, R. M. Caprioli,* Anal. Chem. **71** (1999) 5263.
18. *D. S. Cornett, M. L. Reyzer, P. Chaurand, R. M. Caprioli*, Nature Methods **4** (2007) 827.
19. *B. Spengler, M. Hubert*, J. Am. Soc. Mass Spectrom. **13** (2002) 735.
20. *A. F. M. Altelaar, I. Taban, L. A. McDonnell, P. D. E. M. Verhaert, R. P. J. de Lange, R. A. H. Adan, W. J. Mooi, R. M. A. Heeren, S. R. Piersma,* Int. J. Mass Spectrom. **260** (2007) 203.
21. *P. Chaurand, S. A. Schwartz, D. Billheimer, B. J. Xu, A. Crecelius, R. M. Caprioli,* Anal. Chem. **76** (2004) 1145.
22. *J.-P. Cosyns*, Drug Safety **26** (2003) 33.
23. *H. H. Schmeiser, C. A. Bieler, M. Wiessler, C. van Ypersele de Strihou, J. P. Cosyns*, Cancer Res. **56** (1996) 2025.
24. *A. P. Grollman, S. Shibutani, M. Moriya, F. Miller, L. Wu, U. Moll, N. Suzuki, A. Fernandes, T. Rosenquist, Z. Medverec, K. Jakovina, B. Brdar, N. Slade, R. J. Turesky, A. K. Goodenough., R. Rieger, M. Vukelić, B. Jelaković,* Proc. Natl. Acad. Sci. USA **104** (2007) 12129.
25. *A. P. Grollman, B. Jelakovic*, J. Am. Soc. Nephrol. **18** (2007) 2817.
26. *F. D. Debelle, J. L. Nortier, E. G. De Prez, C. H. Garbar, A. R. Vienne, I. J. Salmon, M. M. Deschodt-Lanckman, J.-L. Vanherweghem*, J. Am. Soc. Nephrol. **13** (2002) 431.
27. *N. Sato, D. Takahashi, S. M. Chen, R. Tsuchiya, T. Mukoyama, S. Yamagata, M. Ogawa, M. Yoshida, S. Kondo, N. Satoh, S. Ueda*, J. Pharm. Pharmacol. **56** (2004) 221.

28. *C. Y. Zhang, X. Wang, M. Y. Shang, J. Yu, Y. Q. Xu, Z. G. Li, L. C. Lei, X. M. Li, S. Q. Cai, T. Namba,* Biomed. Chromatogr. **20** (2006) 309.
29. *N. Kuzushita, A. B. Rogers, N. A. Monti, M. T. Whary, M. J. Park, B. I. Aswad, H. Shirin, A. Koff, H. Eguchi, S. F. Moss,* Gastroenterology **129** (2005) 1544.

List of symbols
Popis simbola

$\overline{d}$ – average diameter, μm
– prosječni promjer, μm

m – molecular mass, Da, kDa
– molekulska masa, Da, kDa

t – time, s
– vrijeme, s

z – charge
– naboj

γ – mass concentration, mg mL^{-1}
– masena koncentracija, mg mL^{-1}

φ – volume fraction, %
– obujmni udjel, %

SAŽETAK

Masena spektrometrija molekulskog oslikavanja

Dj. Josić[a,c] *i S. Kovač*[a,b]

Razvoj masene spektrometrije u posljednjih 20 godina i primjena ove metode u analitici makromolekula, prije svega proteina i ugljikohidrata, otvorio je nove perspektive za uporabu ove metode u medicini, biotehnologiji i ostalim biodisciplinama. Ova se metoda može primijeniti i u novim područjima, kao što su mikroelektronika, geokemija i površinska analitika, posebice nanotehnologija.[1]

Imaging mass spectrometry (IMS) je jedna vrsta sinteze dviju tehnika, histokemije i masene spektrometrije. Ova metoda omogućava optički prikaz rasporeda raspodjele malih i velikih molekula u uzorku, pa čak i makromolekula kao što su proteini i polisaharidi.[2] Optimalizacija masene spektrometrije, ali također i veliki napredak u razvoju instrumentacije dodatni su razlog za sve veći interes za ovu metodu u mnogim interdisciplinarnim područjima medicine, biotehnologije, ali i anorganskim tehnologijama i znanosti o materijalima (*material science*).[1]

Imaging MS daje mogućnost izravnog praćenja prostorne raspodjele molekula u stanicama ili tkivu. Za dobivanje molekularne distribucije u adekvatno pripravljenom uzorku najčešće se primjenjuju Matrix-Assisted Laser Deionisation (MALDI) Time of Flight (TOF) ili Secondary Ion Mass Spectrometry (SIMS)[4]. Pomoću MALDI TOF dobiva se slika prostorne raspodjele velikih molekula, prije svega proteina. Rezolucija ove metode je 25 μm, što je još uvijek nedovoljno da se prati raspored komponenata na razini stanice, ali novi instrumenti omogućavaju i bolju rezoluciju u području od oko 10 μm.

SIMS je metoda koja se primjenjuje za praćenje prostorne raspodjele malih molekula, najčešće biološki aktivnih supstancija.[1,5,6] MALDI TOF je pak metoda izbora za analizu prostorne distribucije makromolekula, najčešće proteina i polipeptida.

IMS se do sada primjenjivala za patološke studije i analizu biomarkera,[3,7–10] za analizu tumora, kao glioblastoma,[3] karcinoma debeloga crijeva,[11] metastaza u jetri,[12] kod praćenja promjena u moždanom tkivu kod Alzheimerove bolesti[10] i ostalih promjena u živčanom tkivu,[14] kod nefrotoksiciteta[13] itd.

Na sl. 1 prikazan je princip određivanja raspodjele makromolekula pomoću MALDI TOF masene spektrometrije. Nakon rezanja tankog sloja i fiksiranja, tkivu se dodaje određena supstancija (matrix) koja omogućava optimalnu ionizaciju i mobilizaciju makromolekula. Vrijeme letenja (time of flight) je obrnuto proporcionalno vrijednosti kvocijenta fragmentirane mase i (pozitivnog) naboja m/z. Računalo automatski upravlja sveobuhvatnim snimanjem površine (screening) i daje površinsku sliku rasporeda molekule određene m/z vrijednosti. To se vidi i na slici 4 koja daje raspodjelu molekule s m/z vrijednosti od 7.791 u uzorku bubrega miša otrovanog aristolohijskom kiselinom I (AA I). Na slici 4 je prikazan raspored triju različitih molekula u istim uzorcima.

Model miša tretiranog s AA I i AA II je izoliran jer postoje opravdani pokazatelji da je kroničnо trovanje ovom suspstancijom jedan od uzroka endemskog nefritisa (EN). Endemski nefritis je kroničnо oboljenje bubrega, proširen u endemskim područjima u donjem toku rijeke Dunava. U Hrvatskoj se ova bolest pojavljuje u određenim selima Brodske Posavine zapadno od Slavonskog Broda.

Bakterija *Helicobacter pylori* je uzročnik infekcije želuca, koja dovodi do kroničnoga gastritisa i, godinama nakon infekcije, do karcinoma. Model miša, inficiranog s *Helicobacter pylori* pokazuje da 15 dana nakon infekcije dolazi do promjene u raspodjeli proteina, i da protein s m/z vrijednos-

ti 9,962 gotovo nestaje s maseno-spekrometrijskog profila. Ovi pokusi su prvi koraci u definiranju molekulskih promjena kod karcinogeneze želuca, definiciji novih biomarkera za otkrivanje rizika i prognozu kod ove zloćudne bolesti.

– IMS je tehnika kojom se kombinira histologija i masena spektrometrija MALDI TOF.

– IMS trenutačno nalazi primjenu u medicini, za identifikaciju kandidata za biomarkere za maligne i druge bolesti.

– Kao tehnika, *imaging mass spectrometry* ima velike perspektive za primjenu u agrikulturi, prehrambenoj tehnologiji i biotehnologiji i to za kontrolu kvalitete i praćenja promjena u biljnim, životinjskim tkivima i mikrobnim stanicama tijekom procesa proizvodnje.

[a] *Sveučilište J. J. Strossmayera u Osijeku, Odjel za kemiju, Kuhačeva 20, 31000 Osijek, Hrvatska*

[b] *Prehrambeno-tehnološki fakultet Osijek, Kuhačeva 18, 31000 Osijek, Hrvatska, e-mail: spomenka.kovac@ptfos.hr*

[c] *Proteomics Core, Center for Cancer Research Development, Rhode Island Hospital and Brown University, Providence, Rhode Island, USA, e-mail: djuro-josic@brown.edu*

Prispjelo 8. prosinca 2008.
Prihvaćeno 3. travnja 2009.